



Preparation of activated carbon using sea mango (*Cerbera odollam*) with microwave-assisted technique for the removal of methyl orange from textile wastewater

Nur Hidayah Azmi^a, Umi Fazara Md. Ali^{a,*}, Fahmi Muhammad Ridwan^a,
Khairuddin Md Isa^a, Nurul Zufarhana Zulkurnai^a, Mohamed Kheireddine Aroua^b

^aSchool of Environmental Engineering, University Malaysia Perlis, Kompleks Pusat Pengajian Jejawi 3, Arau, Perlis 02600, Malaysia, emails: hiazmee_88@yahoo.com.my (N.H. Azmi), unifazara@unimap.edu.my (U.F.M. Ali), drfahmi@unimap.edu.my (F. Muhammad Ridwan), khairudin@unimap.edu.my (K.M. Isa), nurulzufarhana@yahoo.com (N.Z. Zulkurnai)

^bFaculty of Engineering, Department of Chemical Engineering, University Malaya, Lembah Pantai, Kuala Lumpur 50603, Malaysia, email: mk_aroua@um.edu.my

Received 2 September 2015; Accepted 10 March 2016

ABSTRACT

Sea mango (*Cerbera odollam*), a non-edible fruit which is abundantly available in Malaysia was transformed into a potential low-cost activated carbon for the removal of methyl orange (MO) (mono azo dye) from textile wastewater. The activated carbon was subjected to carbonization process at 200°C with nitrogen (N₂), followed by chemical activation with phosphoric acid (H₃PO₄) and physical activation using microwaves at 500°C for 2 h. The Brunauer–Emmet and Teller surface area for the produced activated carbon was 1,437 m²/g. The effects of several operating parameters, such as activated carbon dosage, contact time; initial concentration, and pH at room temperature on the adsorption process of MO from simulated textile wastewater were evaluated. The minimum duration for the dye adsorption reached the equilibrium state was 60 min. Removal of dye in acidic solutions was preferred rather than in basic solution. Higher initial dye concentration performed better on dye removal than lower concentration. Adsorption behavior of MO on sea mango activated carbon was expressed by both Langmuir and Freundlich isotherms.

Keywords: Sea mango (*Cerbera odollam*); Activated carbon; Methyl orange; Phosphoric acid; Microwaves; Isotherms

1. Introduction

Industrial effluent from various industries such as textile, plastics, paper, and dyestuffs produced a bulky

amount of wastewater per day. Approximately 2% of dyes are released directly to the effluent during the manufacturing processes and nearly 10% of the dye loss throughout coloration process in textile industries [1]. Dye color is the main pollutant identified in wastewater, which is a significance of incompetent

*Corresponding author.

processing both in the dye-consuming and manufacturing industries. The toxicity and existence of this color in very little amounts in water is highly visible and unpleasant for aquatic life.

In recent years, a number of techniques have been utilized on dyes treatment such as photocatalytic degradation [2–4], electrocoagulation [5,6], electrochemical [7], advanced oxidation process [8], and membrane separation [9,10], but these methods are found to be impracticable in terms of cost and implementation. This commenced researchers to discover cost-effective methods for dye removal such adsorption technique by carbon adsorbent. Adsorption process using activated carbon is suitable in removing soluble impurities from wastewater like methyl orange (MO) dye as it can be absolutely removed even from the diluted solution. The activated carbon itself has large surface area per unit volume (m^2/g) which consists of meso and micropore where adsorption takes place. It is the superior procedure and proved the best result among the various methods of dye removal and can be used for other types of pollutants [11–14] as well.

The adsorption efficiency of the activated carbon is really depend on the physical properties such as total surface area, bulk density, hardness, and chemical properties included pH [15], temperature, and initial concentration of adsorbate. The characterization through isotherm was performed in order to know the capacity adsorption of the adsorbent. A few reviews related to the isotherm studies of MO on adsorbent were done [1,16–21]. It was found that various isotherm models have been fitted to represent the data. There are a few of parameter model, which are Freundlich, Langmuir, Redlich–Peterson, Radke–Prausnitz, and Toth. Of these, Freundlich and Langmuir model have been mostly used of the adsorbents for MO adsorption isotherm.

Adsorbents such as spent tea leaves [22], mango bark [23], coffee husks [24], coffee waste [25], cotton waste [14], and eggshells [26] have been studied widely as adsorbents. After a detailed screening in literature, there is no review articles focused on using the natural material for dye removal. In the present research, the activated carbon will be produced using the sea mango (*Cerbera odollam*) which is a non-commercialize precursor using three steps which are carbonization with flow of nitrogen gas (N_2), impregnation in phosphoric acid (H_3PO_4), and activation with absence of any gas. The main goal of this study is to generate the best quality of activated carbon using sea mango which able to adsorb the highest amount of MO in the wastewater.

2. Materials and methods

2.1. Materials

Phosphoric acid (H_3PO_4) and MO were supplied from Merck Milipore Corporation (80.0% purity, Darmstadt, Germany) and Sigma-Aldrich (M) Sdn. Bhd (Kuala Lumpur, Malaysia), respectively. The precursor for the activated carbon was from the non-edible fruit; sea mango (*c. odollam*), which was collected from Perlis, Malaysia.

2.2. Synthesis of sea mango activated carbon (SMAC)

Mesoporous activated carbon was synthesized using sea mango raw material (SMRM) as described by Hidayah et al. [27]. In a typical preparation, the fibrous shell part with particle size of 1–2 mm was carbonized at 200°C for 30 min with the presence of nitrogen gas. Then, the sample was impregnated with H_3PO_4 with mass ratio of 1:2 (precursor to activating agent) and was then dried overnight in the oven at 110°C under static condition. Subsequently, the mixture was heated at 500°C using microwave energy at a rate of 1.5 L/min. After completing a duration of 2 h, the sample was washed several times with hot distilled water to remove excessive H_3PO_4 . The activated carbon was then dried and maintained in an air-tight container. The produced SMAC was ready to be used.

2.3. Characterization of activated carbon

The surface features of activated carbon prepared were verified using the nitrogen sorption technique. The nitrogen adsorption/desorption isotherms were obtained from Micromeritics ASAP 2020 analyzer (Micromeritics Instrument Corporation, Norcross, GA, USA) and measured at -196°C . Prior to adsorption/desorption process, the samples were degassed for 3 h at 300°C. The specific surface area was determined according to the Brunauer–Emmet–Teller (BET) model [28], while the pore structure of the activated carbon sample was analyzed using the Barrett–Joyner–Halenda method [29].

A Fourier transform infrared (FTIR) spectrometer (model 1600, PerkinElmer, Waltham, MA, USA) was used to identify the surface functional groups. Activated carbon sample was mixed with spectroscopic-grade KBr and formed into pellets at a pressure of approximately 1 MPa. The samples were scanned in the spectral range between 4,000 and 400 cm^{-1} .

Scanning electron micrograph (SEM) (model TM3000, Hitachi High-Technologies Corporation, Tokyo, Japan) was employed to examine morphologies

structure on SMRM and SMAC. Prior to inspection, the biomass samples were coated with a thin electrical conductive platinum film using an auto-fine coater (model JFC-1600, JEOL Ltd, Tokyo, Japan).

2.4. Adsorption studies

Batch studies were performed at the room temperature to evaluate the effect of various parameters (adsorbent dosage, solution pH, contact time, and initial concentration) for the removal of MO on SMAC from aqueous solution. Prior to the experiments, the stock solution was prepared by dissolving 1 g of MO in 1,000 mL of distilled water. In all experiments except for the initial concentration, weighted SMAC was added to 100 mL of adsorbate solution with a concentration of 50 mg/L. Subsequently, the flasks that contain adsorbent and adsorbate mixture were employed on the orbital shaker and operated at constant speed of 200 rpm for predetermined time intervals. The residual concentration of MO solution was identified by UV–visible spectrophotometer (model U2801, Hitachi High-Technologies Corporation, Tokyo, Japan) via a calibration curve at maximum wavelength (465 nm). The amount of adsorbed dye, q_e (mg/g) was calculated by:

$$q_e = (C_o - C_e) \cdot \frac{v}{m} \quad (1)$$

where C_o and C_e are the initial and equilibrium liquid-phase dye concentrations (mg/L), respectively, V is the volume of the adsorbate solution (L), and W is the weight of the SMAC adsorbent used (g). The performances of SMAC on dye removal were calculated from the different between the initial and equilibrium concentration of the solution. The effect of adsorbent dosage was studied by varying weight of adsorbent from 0.2 to 1.0 g, whereas a pH range of 3–9 was applied for the effect of pH solution on solid–liquid adsorption studies. The dilution of 0.1 M NaOH and 0.1 M HCl solution was used for pH adjustment [30].

3. Result and discussion

3.1. Characterization of activated carbon

3.1.1. Nitrogen adsorption–desorption isotherms of SMAC

As shown in Fig. 1, the N_2 adsorption and desorption isotherm of SMAC was in agreement with type IV sorption isotherm and type H4 hysteresis loops

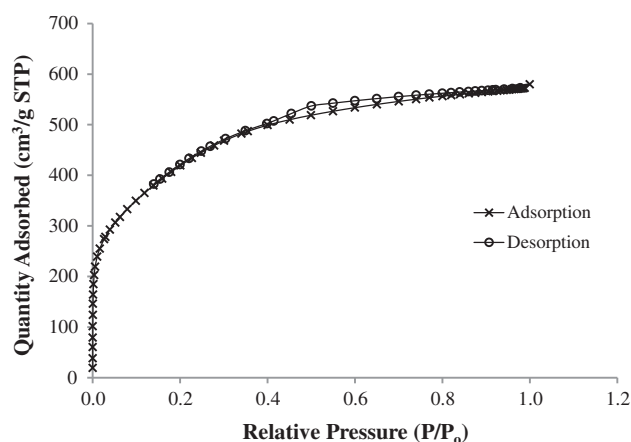


Fig. 1. Nitrogen adsorption–desorption isotherm.

profiles, according to the IUPAC classification [31]. Type IV sorption isotherm and H4 hysteresis loops show the concurrent existence of micro and mesopores. The initial part at (0.0–0.01) relative pressure indicates the result of monolayer–multilayer adsorption on the mesopore walls [32]. Porous structure results showed a high quality of activated carbon was successfully derived with surface area of 1,437 m²/g with the total pore volume (V_t) and mesoporous volume (V_{meso}) are 0.897 and 0.885 cm³/g, respectively, which signifying that it is mainly the mesoporous structure. The adsorbent pores were classified by IUPAC into three categories: micropore width (<2 nm), mesopore width (2–50 nm), and macropore width (>50 nm) [33].

3.1.2. Functional groups of SMRM and SMAC

The spectral peaks in both samples SMRM and SMAC contain a number of functional groups, (Fig. 2). SMRM and SMAC have different spectrum peaks of Fourier transform infrared spectra (FTIR) as these peaks may have shifted, decreased in size or completely removed during activation. By comparing with SMRM spectral peaks, there are three peaks have shifted and existence permanently for SMAC at O–H stretching of hydroxyl group (3,368 cm⁻¹), C=C of aromatic ring (1,567 cm⁻¹), and C–O ether (1,061 cm⁻¹).

Raw sea mango showed a complex FTIR spectrum which indicated surface functional group of the lignocellulosic material. At peak 3,339 cm⁻¹ showed a strong and broad absorption indicated the O–H stretching vibration of hydroxyl functional groups, including intermolecular hydrogen bonding [34]. Alkane functional group with C–H sp^3 stretching bond was observed at peak 2,920 cm⁻¹. Furthermore, carbonyl (C=O stretching) and aromatic (C=C stretching) were

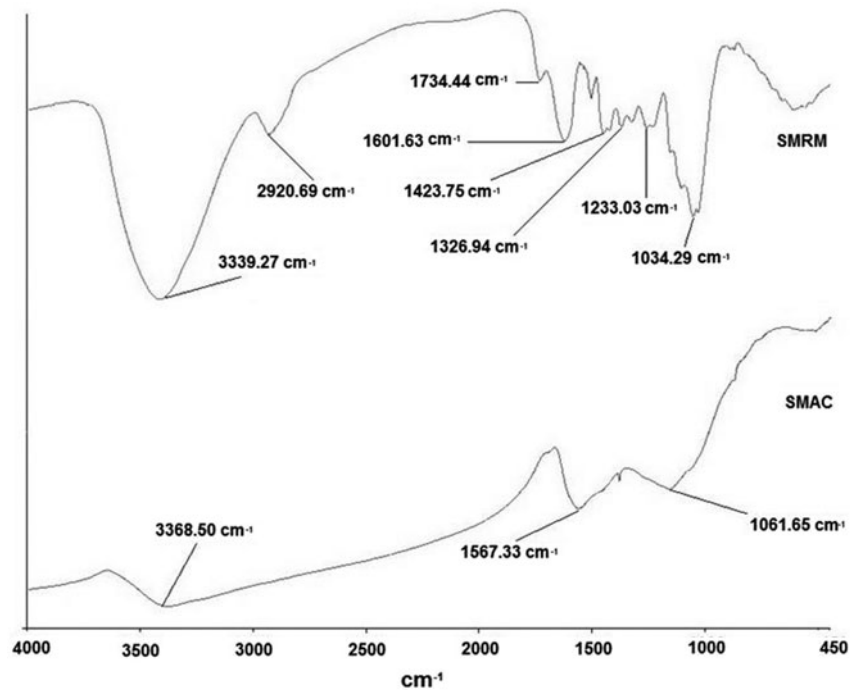


Fig. 2. FTIR spectra for SMRM and SMAC.

found at peak 1,734 and 1,601 cm^{-1} , respectively. Besides, two peaks that indicated alkane group with C–H bending were observed at peak 1,423 and 1,326 cm^{-1} . On other hand, C–O stretching that indicated ethers functional groups was found with double peak at 1,233 and 1,034 cm^{-1} spectrum. Through all the peaks produced by IR spectra, indicated that SMRM functional group had similar as cerberin structure (Fig. 3). The absorption frequencies and functional group of SMRM and SMAC are summarized in Table 1.

3.1.3. Surface morphologies of SMRM and SMAC

Results of SEM of the SMRM and SMAC are illustrated in Fig. 4, which on the similar top rod-like

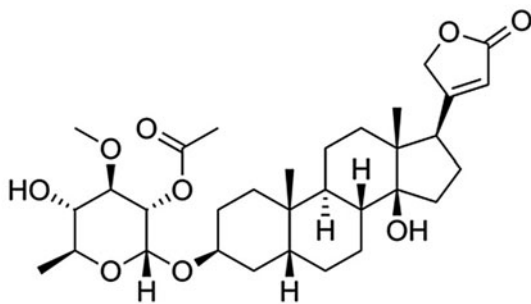


Fig. 3. Chemical structure of cerberin.

part for both samples were compared. SMRM image showed lignocellulosic structure and existence of porous structure on SMAC image after undergoing physicochemical treatment. Chemical treatment using H_3PO_4 was created cavities on the carbon surface and most organic matter easily evolved at higher temperature of 500 $^\circ\text{C}$ during physical treatment. The development of porous structure on carbon surface were proved that chemical and physical treatments applied were successfully produced a good carbon adsorbent for liquid adsorption. Liquid molecule would attach on pore structure through physisorption during adsorption process.

3.2. Study of various parameters on the adsorption of MO dye by SMAC

3.2.1. Effect of adsorbent dosage

The effect of adsorbent dose on removal of MO was studied by varying the adsorbent dosage while keeping the same initial dye concentration. Fig. 5 reveals that percent of dye removal was increased as the increasing of adsorbent dosage. At stable condition, the percentage of removal enhanced from 65 to 80% for an increase in SMAC dosage from 0.2 to 0.4 g. However, after the critical dosage of 0.6 g, the adsorption percentage achieved a constant value with 100% of dye removal. The increased of dye removal

Table 1
Absorption frequencies and functional groups for SMRM and SMAC

Functional group	Molecular motion	Absorption Frequency (cm^{-1})	Peak (cm^{-1})	
			SMRM	SMAC
Alcohol	O–H stretch	3,200–3,600	3,339	3,368
Alkane	C–H stretch	2,850–3,000	2,920	–
Carbonyl	C=O stretch	1,670–1,820	1,734	–
Aromatic	C=C stretch	1,400–1,620	1,601	1,567
Alkane	–C–H bend	1,350–1,480	1,423, 1,326	–
Ether	C–O stretch	1,000–1,320	1,233, 1,034	1,061

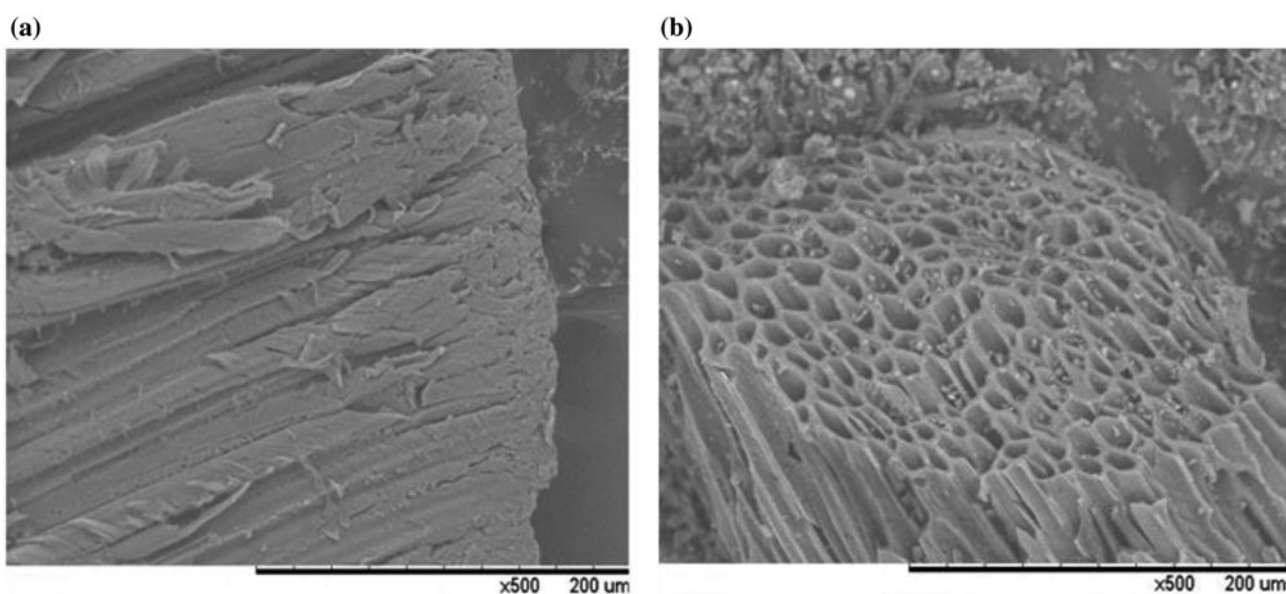


Fig. 4. Surface structure through SEM image for (a) SMRM and (b) SMAC.

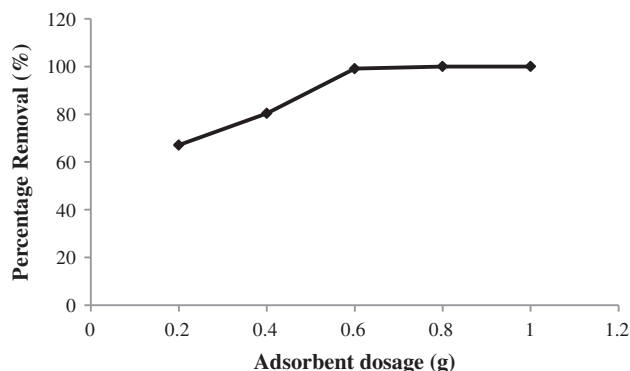


Fig. 5. Effect of adsorbent dosage on the adsorption of MO on SMAC (initial dye concentration: 50 mg/L, Volume = 100 mL, $T = 25^\circ\text{C}$).

percentage was due to the availability of the active site surface [35,36]. However, during the increasing of adsorbent dosage to 0.8 g, the trend showed no significance differences, as the surface site reach the maximum availability of carbon dosage to the adsorbate concentration.

3.2.2. Effect of pH

The pH value is one of the main important parameter that gives a great effect to the removal of the MO. As shown in Fig. 6, the amount adsorption of adsorbate reduced with the increasing of pH. When the pH was changed from 3 to 9, the adsorption yield reduced from 25 to 18 mg/g. On the other hand, the adsorption capacity was changed about 21% from pH 5 to 7. It was proven that acidic was the best condition in

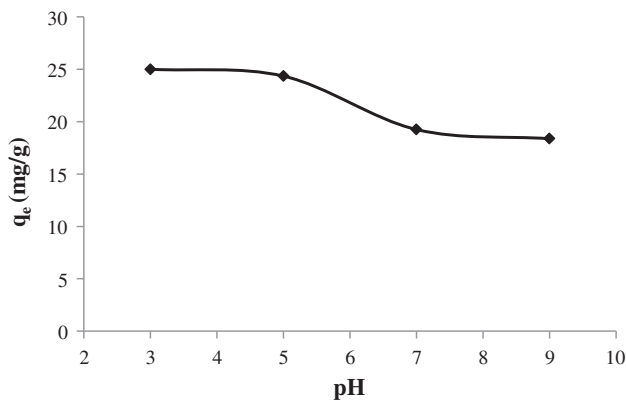


Fig. 6. Effect of pH on the removal of MO dye by SMAC (initial dye concentration: 50 mg/L, SMAC dosage: 0.2 g/100 mL, $T = 25^\circ\text{C}$).

removal of MO, due to the rich of H^+ ions on the adsorbent surface with more attraction to MO molecule with anionic charge. The different charge of adsorbent and adsorbate will enhance the ability of adsorption of MO onto SMAC. The similar result was recorded by Chen and co-workers [32]. In contrast, Hamdaoui and Naffrechoux [37] reported that OH^- ions cause repulsion between negatively charge surface and the dye molecule. According to Hameed [38], the adsorbent may receive negatively charge cause by the higher pH solution of adsorbate which enhance the positively charge dye cation through electrostatic force of attraction.

3.2.3. Effect of contact time

As illustrated in Fig. 7, it is apparent that time has essential influence on the adsorption of dye for a variety of initial dye concentrations (50, 100, 150, 200, and 250 mg/L). Every single concentration showed similar pattern of dye adsorption with slightly expeditious in the first 30 min, subsequently slowly increased with the extension of contact time except for the lowest initial concentration (50 mg/L). After 60 min of contact time, no noticeable variation in adsorbed dye was detected. At the earlier contact time, rapid increasing of percentage removal occurs because of the availability of surface of activated carbon with positive charge. On the other hand, the slow rate of adsorption after the equilibrium condition reached is due to the slow pore diffusion of the solute ion into the bulk of the adsorbent [32]. Nevertheless, there was no significant influence on the adsorption of dye for the lowest initial concentration of 50 mg/L.

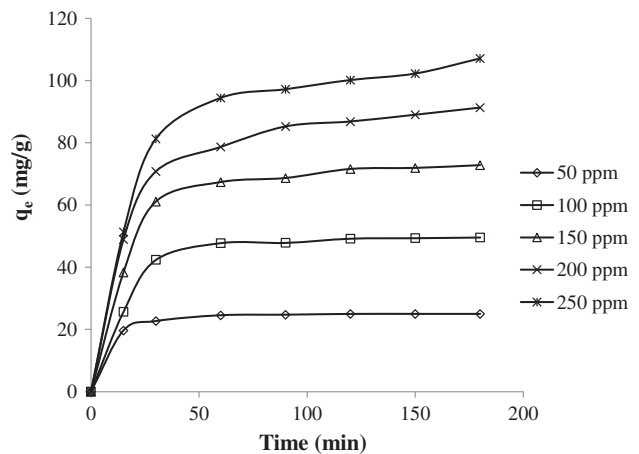


Fig. 7. Effect of contact time on the removal of MO dye by SMAC (initial dye concentration: 50, 100, 150, 200, and 250 mg/L, SMAC dosage: 0.2 g/100 mL, $T = 25^\circ\text{C}$).

3.2.4. Effect of initial dye concentration

The effect of the initial dye concentration on the adsorption capacity and dye removal efficiency is illustrated in Fig. 8. It was observed that dye removal efficiency reached up to maximum of 98% at the lowest concentration (50 mg/L), then reduced to 78% at the highest concentration (250 mg/L). It was proved that availability unoccupied binding sites on the adsorbents was limited for low initial concentration as compared to high initial concentration. The capacity of dye adsorbed enhanced from 25 to 97 mg/g with an increment in the initial dye concentration from 50 to 250 mg/L. The essential driving force was provided by initial dye concentration to overcome the resistance due to interchanging of dye molecule between

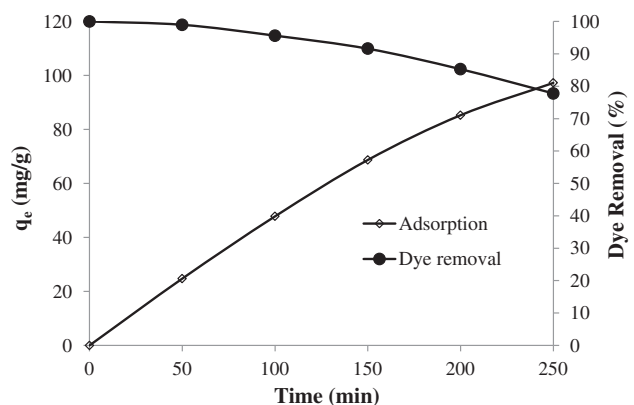


Fig. 8. Effect of initial dye concentration on the removal of MO dye by SMAC (SMAC dosage: 0.2 g/100 mL, $T = 25^\circ\text{C}$).

aqueous and solid phases. As a result, the interaction between MO and SMAC adsorbent was increased, and the initial dye concentration was also increased.

3.3. Isotherm analysis

The equilibrium of adsorption was determined using the Langmuir and the Freundlich isotherms to describe the adsorption behavior of the solid–liquid system. The Langmuir isotherms theory showed the relationship between the active sites of the surface undergoing the adsorption process [22], whereas adsorbate with monolayer features coverage on the top of homogenous adsorbent surface. A basic supposition is that sorption process occurs at definite homogenous sites within the adsorbent. After a dye molecule engaged the empty site, no more adsorption can occur at that site.

The basic Langmuir model is:

$$q_e = \frac{Q_m K_L C_e}{1 + K_L C_e} \tag{2}$$

The model generally was simplified into the form by the following equation:

$$\frac{C_e}{q_e} = \frac{1}{Q_m K_L} + \frac{1}{Q_m} C_e \tag{3}$$

where C_e is the equilibrium concentration of the adsorbate (mg/L), q_e is the amount of adsorbate adsorbed per unit mass of adsorbent (mg/g), Q_m is the theoretical maximum adsorption capacity (mg/g), and K_L (L/mg) is the Langmuir isotherm constant related to adsorption efficiency and energy of adsorption, respectively. The linear plot of c_e/q_e against c_e followed a Langmuir isotherm model as in Fig. 9. Q_m and K_L were obtained from the slope and intercept of the plot. The equilibrium data and constant for the Langmuir isotherm is listed in Table 2. The dimensionless constant separation factor, R_L that is given by Eq. (4) which is defined as follows:

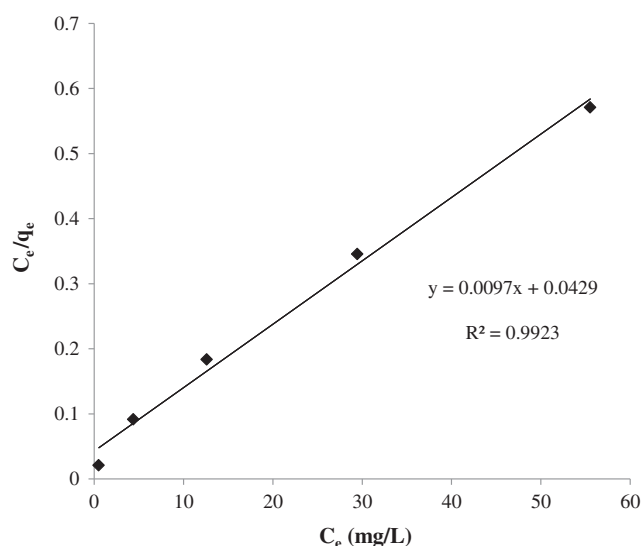


Fig. 9. Langmuir isotherm for adsorption of MO on SMAC.

$$R_L = \frac{1}{1 + K_L C_o} \tag{4}$$

where C_o is the initial dye concentration (mg/L) and K_L (L/mg) is the Langmuir constant. By referring the R_L value, the shape of the isotherm was divided into four shapes to be either unfavorable ($R_L > 1$), linear ($R_L = 1$), favorable ($0 < R_L < 1$), or irreversible ($R_L = 0$). In this present study, the value of R_L for the adsorption of MO onto SMAC is in the range of 0.01–0.08, indicated that the adsorption was a favorable process (Fig. 10).

The Freundlich isotherm is an empirical equation assuming that the adsorption process ensued on the homogenous surfaces and the concentration of MO dye at equilibrium condition is related to its adsorption capacity. On other hand, this type of isotherm was taken heterogeneous system into account and is not limited to the formation of the monolayer [39].

The basic Freundlich isotherm is:

$$q_e = K_F C_e^{1/n} \tag{5}$$

Table 2
Isotherm constant value for MO adsorption on SMAC

Langmuir				Freundlich		
Q_m (mg/g)	K_L (L/mg)	R_L	R^2	K_F (L/mg)	$1/n$	R^2
103.10	0.2261	0.01–0.08	0.9923	30.70	0.2983	0.9959

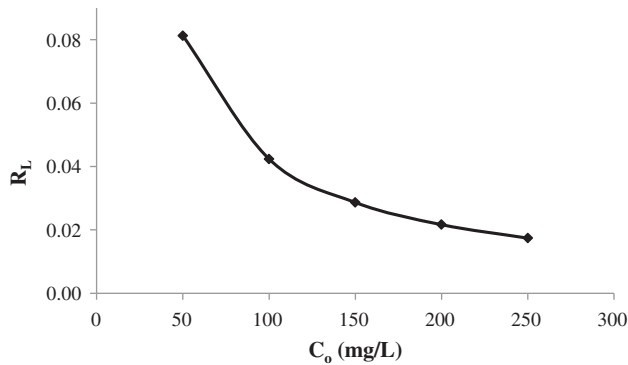


Fig. 10. The separation factor for MO adsorption on SMAC.

The model was simplified into the normal form by the following equation:

$$\ln q_e = \ln K_F + \frac{1}{n} \ln C_e \quad (6)$$

The adsorption capacity is approximately indicated by K_F (L/mg), while adsorption intensity and surface heterogeneity measured by $1/n$. The scale of the exponent, $1/n$, showed the favorability of adsorption where value $n > 1$ correspond to favorable adsorption condition. It becomes more heterogeneous as its $1/n$ value gets closer to zero. Table 2 lists the value of K_F and the linear regression correlation (R^2) that was obtained from plotted graph at Fig. 11 for the Freundlich isotherm.

As presented in the table, Freundlich isotherm with R^2 value of 0.9959 constitutes a better fit of experimental data than the Langmuir isotherm with R^2 value of 0.9923. It signifies that Freundlich isotherm appears to produce a reasonable model for sorption with the value of $1/n$ was found between 0 and 1 representing high adsorption intensity. The amount of

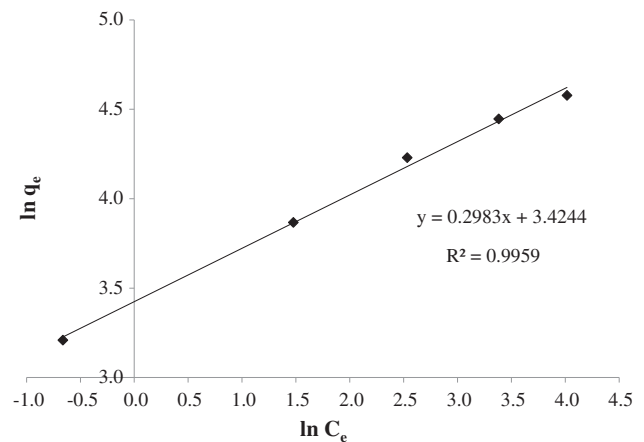


Fig. 11. Freundlich isotherm for adsorption of MO on SMAC.

computed maximum monolayer capacity of SMAC for the removal of MO by the Langmuir model was found to be 103.10 mg/g.

3.4 Comparative study

The comparison of experimental adsorption capacity of SMAC obtained in this study with those reported in the literature using assorted adsorbents is presented in Table 3. The experimental results revealed the suitable adsorption capacity of SMAC in removal of MO dye. The maximum adsorption capacity, Q_m of MO onto SMAC is comparatively higher than some materials, whereas lower than the slightly costly adsorbents such as carbon-coated monolith. Additionally, the abundantly available of SMAC raw material, sea mango can be used as promising material to minimize the concentration of MO from aqueous solution.

Table 3

Adsorption capacities for the removal of MO by other alternative adsorbents and this study

Adsorbent	Dye	Adsorption capacity (mg/g)	Refs.
Modified wheat straw	MO	50.4	[40]
Modified coffee waste	MO	58.8	[25]
Bottom ash	MO	3.6	[41]
De-oiled soya	MO	16.7	[41]
Banana peel	MO	21.0	[42]
Orange peel	MO	20.5	[42]
Carbon-coated monolith	MO	147.1	[43]
SMAC (sea mango)	MO	103.1	This study

4. Conclusion

Sea mango from the new precursor from the ornamental plant waste showed a very good characteristic in terms of surface area (BET), surface morphology (SEM), and FTIR results. The performance of activated carbon produced was tested via the removal of MO from aqueous solution. The result obtained proved that the surface area of the activated carbon was relatively high (1,437 m²/g) showed high potential to be used as an adsorbent. The batch experiment showed that adsorption process occurred rapidly, as the highest removal occurred within 50 min of contact time and the adsorption capacity of MO dye was better in acidic condition. The adsorption of dye enhanced with the increasing of initial dye concentration. The equilibrium data for adsorption parameters for the Langmuir and Freundlich were determined and the best adsorption isotherm with the highest regression described by the Freundlich isotherm model with linear regression (0.9959). The sea mangos used in this present work are freely and abundantly available with promises low-cost adsorbent for the removal of MO from aqueous solution that was suitable for the textile industries.

Acknowledgments

The authors are grateful for financial support provided by the Research Acculturation Collaborative Effort (RACE) and Program Rakan Penyelidikan UM Grant (CR001-2014), which made this research possible.

References

- [1] A. Mittal, J. Mittal, A. Malviya, D. Kaur, V.K. Gupta, Decoloration treatment of a hazardous triarylmethane dye, light green SF (Yellowish) by waste material adsorbents, *J. Colloid Interface Sci.* 342 (2010) 518–527.
- [2] V.K. Gupta, R. Jain, A. Mittal, T.A. Saleh, A. Nayak, S. Agarwal, S. Sikarwar, Photo-catalytic degradation of toxic dye amaranth on TiO₂/UV in aqueous suspensions, *Mater. Sci. Eng. C* 32 (2012) 12–17.
- [3] T.A. Saleh, V.K. Gupta, Photo-catalyzed degradation of hazardous dye methyl orange by use of a composite catalyst consisting of multi-walled carbon nanotubes and titanium dioxide, *J. Colloid Interface Sci.* 371 (2012) 101–106.
- [4] V.K. Gupta, R. Jain, A. Nayak, S. Agarwal, M. Shrivastava, Removal of the hazardous dye—Tartrazine by photodegradation on titanium dioxide surface, *Mater. Sci. Eng. C* 31 (2011) 1062–1067.
- [5] S. Vasudevan, J. Lakshmi, G. Sozhan, Optimization of electrocoagulation process for the simultaneous removal of mercury, lead, and nickel from contaminated water, *Environ. Sci. Pollut. Res.* 19 (2012) 2734–2744.
- [6] K.-W. Pi, Q. Xiao, H.-Q. Zhang, M. Xia, A.R. Gerson, Decolorization of synthetic methyl orange wastewater by electrocoagulation with periodic reversal of electrodes and optimization by RSM, *Process Saf. Environ. Prot.* 92 (2014) 796–806.
- [7] V.K. Gupta, R. Jain, S. Varshney, Electrochemical removal of the hazardous dye reactofix red 3 BFN from industrial effluents, *J. Colloid Interface Sci.* 312 (2007) 292–296.
- [8] M. Brienza, M. Mahdi Ahmed, A. Escande, G. Plantard, L. Scrano, S. Chiron, S.A. Bufo, V. Goetz, Use of solar advanced oxidation processes for wastewater treatment: Follow-up on degradation products, acute toxicity, genotoxicity and estrogenicity, *Chemosphere* 148 (2016) 473–480.
- [9] K. Majewska-Nowak, J. Kawiecka-Skowron, Ceramic membrane behaviour in anionic dye removal by ultrafiltration, *Desalin. Water Treat.* 34 (2011) 367–373.
- [10] M.F. Abid, M.A. Zablouk, A.M. Abid-Alameer, Experimental study of dye removal from industrial wastewater by membrane technologies of reverse osmosis and nanofiltration, *Iran. J. Environ. Health Sci. Eng.* 9 (2012) 1–9.
- [11] V.K. Gupta, S.K. Srivastava, D. Mohan, S. Sharma, Design parameters for fixed bed reactors of activated carbon developed from fertilizer waste for the removal of some heavy metal ions, *Waste Manage. (Oxford)* 17 (1998) 517–522.
- [12] V.K. Gupta, B. Gupta, A. Rastogi, S. Agarwal, A. Nayak, Pesticides removal from waste water by activated carbon prepared from waste rubber tire, *Water Res.* 45 (2011) 4047–4055.
- [13] V.K. Gupta, S. Agarwal, T.A. Saleh, Synthesis and characterization of alumina-coated carbon nanotubes and their application for lead removal, *J. Hazard. Mater.* 185 (2011) 17–23.
- [14] J.N. Bhakta, P.B. Majumdarand Yukihiro Munekage, Development of activated carbon from cotton fibre waste as potential mercury adsorbent: Kinetic and equilibrium studies, *Int. J. Chem. Eng.* 2014 (2014) 1–7.
- [15] U.F.M. Ali, Removal of Ash from Palm-Shell-Based Activated Carbon Using Acid Blends Kuala Lumpur, University of Malaya, Kuala Lumpur, 2005.
- [16] A. Mittal, D. Kaur, A. Malviya, J. Mittal, V.K. Gupta, Adsorption studies on the removal of coloring agent phenol red from wastewater using waste materials as adsorbents, *J. Colloid Interface Sci.* 337 (2009) 345–354.
- [17] A. Mittal, J. Mittal, A. Malviya, V.K. Gupta, Adsorptive removal of hazardous anionic dye “Congo red” from wastewater using waste materials and recovery by desorption, *J. Colloid Interface Sci.* 340 (2009) 16–26.
- [18] V.K. Gupta, A. Nayak, Cadmium removal and recovery from aqueous solutions by novel adsorbents prepared from orange peel and Fe₂O₃ nanoparticles, *Chem. Eng. J.* 180 (2012) 81–90.
- [19] V.K. Gupta, M. Gupta, S. Sharma, Process development for the removal of lead and chromium from aqueous solutions using red mud—An aluminium industry waste, *Water Res.* 35 (2001) 1125–1134.
- [20] A. Mittal, J. Mittal, A. Malviya, V.K. Gupta, Removal and recovery of chrysoidine Y from aqueous solutions by waste materials, *J. Colloid Interface Sci.* 344 (2010) 497–507.

- [21] V.K. Gupta, I. Ali, Removal of DDD and DDE from wastewater using bagasse fly ash, a sugar industry waste, *Water Res.* 35 (2001) 33–40.
- [22] B.H. Hameed, Spent tea leaves: A new non-conventional and low-cost adsorbent for removal of basic dye from aqueous solutions, *J. Hazard. Mater.* 161 (2009) 753–759.
- [23] R. Srivastava, D.C. Rupainwar, A comparative evaluation for adsorption of dye on neem bark and mango bark powder, *Indian. J. Chem. Technol.* 18 (2011) 67–75.
- [24] L.S. Oliveira, A.S. Franca, T.M. Alves, S.D.F. Rocha, Evaluation of untreated coffee husks as potential biosorbents for treatment of dye contaminated waters, *J. Hazard. Mater.* 155 (2008) 507–512.
- [25] R. Lafi, A. Hafiane, Removal of methyl orange (MO) from aqueous solution using cationic surfactants modified coffee waste (MCWs), *J. Taiwan Inst. Chem. Eng.* 58 (2016) 424–433.
- [26] R. Slimani, I. El Ouahabi, F. Abidi, M. El Haddad, A. Regti, M.R. Laamari, S.E. Antri, S. Lazar, Calcined eggshells as a new biosorbent to remove basic dye from aqueous solutions: Thermodynamics, kinetics, isotherms and error analysis, *J. Taiwan Inst. Chem. Eng.* 45 (2014) 1578–1587.
- [27] A.N. Hidayah, M.A.U. Fazara, Z.N. Fauziah, M.K. Aroua, Preparation and characterization of activated carbon from the sea mango (*Cerbera odollam*) with impregnation in phosphoric acid (H_3PO_4), *ASEAN J. Chem. Eng.* 15 (2015) 22–30.
- [28] S. Brunauer, P.H. Emmett, E. Teller, Adsorption of gases in multimolecular layers, *J. Am. Chem. Soc.* 60 (1938) 309–319.
- [29] E.P. Barrett, L.G. Joyner, P.P. Halenda, The determination of pore volume and area distributions in porous substances. I. Computations from nitrogen isotherms, *J. Am. Chem. Soc.* 73 (1951) 373–380.
- [30] O.S. Bello, M.A. Ahmad, T.T. Siang, Utilization of cocoa pod husk for the removal of remazol black B reactive dye from aqueous solution: Kinetic, equilibrium and thermodynamic studies, *Trends Appl. Sci. Res.* 6 (2011) 794–812.
- [31] K.S.W. Sing, Reporting physisorption data for gas/solid systems with special reference to the determination of surface area and porosity, *Pure Appl. Chem.* 57 (1985) 603–619.
- [32] S. Chen, J. Zhang, C. Zhang, Q. Yue, Y. Li, C. Li, Equilibrium and kinetic studies of methyl orange and methyl violet adsorption on activated carbon derived from phragmites australis, *Desalination* 252 (2010) 149–156.
- [33] D.H. Everett, Manual of symbols and terminology for physicochemical quantities and units, appendix II: Definitions, terminology and symbols in colloid and surface chemistry, *Pure Appl. Chem.* 31 (1972) 577–638.
- [34] M.A. Fox, J.K. Whitesell, *Organic Chemistry*, Jones & Bartlett Learning Publication, Burlington, 2004.
- [35] N. Kannan, M.M. Sundaram, Kinetics and mechanism of removal of methylene blue by adsorption on various carbons—A comparative study, *Dyes Pigm.* 51 (2001) 25–40.
- [36] V.K. Garg, R. Gupta, A. Bala Yadav, R. Kumar, Dye removal from aqueous solution by adsorption on treated sawdust, *Bioresour. Technol.* 89 (2003) 121–124.
- [37] O. Hamdaoui, E. Naffrechoux, Modeling of adsorption isotherms of phenol and chlorophenols onto granular activated carbon Part I. Two-parameter models and equations allowing determination of thermodynamic parameters, *J. Hazard. Mater.* 147 (2007) 381–394.
- [38] B.H. Hameed, Equilibrium and kinetic studies of methyl violet sorption by agricultural waste, *J. Hazard. Mater.* 154 (2008) 204–212.
- [39] N. Mohammadi, H. Khani, V.K. Gupta, E. Amereh, S. Agarwal, Adsorption process of methyl orange dye onto mesoporous carbon material—kinetic and thermodynamic studies, *J. Colloid Interface Sci.* 362 (2011) 457–462.
- [40] Y. Su, Y. Jiao, C. Dou, R. Han, Biosorption of methyl orange from aqueous solutions using cationic surfactant-modified wheat straw in batch mode, *Desalin. Water Treat.* 52 (2014) 6145–6155.
- [41] A. Mittal, A. Malviya, D. Kaur, J. Mittal, L. Kurup, Studies on the adsorption kinetics and isotherms for the removal and recovery of methyl orange from wastewaters using waste materials, *J. Hazard. Mater.* 148 (2007) 229–240.
- [42] G. Annadurai, R.-S. Juang, D.-J. Lee, Use of cellulose-based wastes for adsorption of dyes from aqueous solutions, *J. Hazard. Mater.* 92 (2002) 263–274.
- [43] W. Cheah, S. Hosseini, M.A. Khan, T.G. Chuah, T.S.Y. Choong, Acid modified carbon coated monolith for methyl orange adsorption, *Chem. Eng. J.* 215–216 (2013) 747–754.